

Supporting Information

Asymmetric tin-vanadium redox electrolyte for hybrid energy storage with nanoporous carbon electrodes

Juhan Lee,^{a,b} Aura Tolosa,^{a,b} Benjamin Krüner,^{a,b} Nicolas Jäckel,^{a,b}
Simon Fleischmann,^b Marco Zeiger,^{a,b} Daekyu Kim,^{a,c} Volker Presser^{a,b,*}

^a INM – Leibniz Institute for New Materials, Campus D2 2, 66123 Saarbrücken, Germany

^b Department of Materials Science and Engineering, Saarland University, Campus D2 2, 66123 Saarbrücken, Germany

^c School of Energy, Materials and Chemical Engineering, Korea University of Technology and Education, Chungjeol-ro 1600, 31253 Cheonan, Republic of Korea

* Corresponding author's eMail: volker.presser@leibniz-inm.de

Electrochemical performance of the $\text{SnSO}_4\text{-VOSO}_4$ redox electrolyte system with activated carbon electrodes

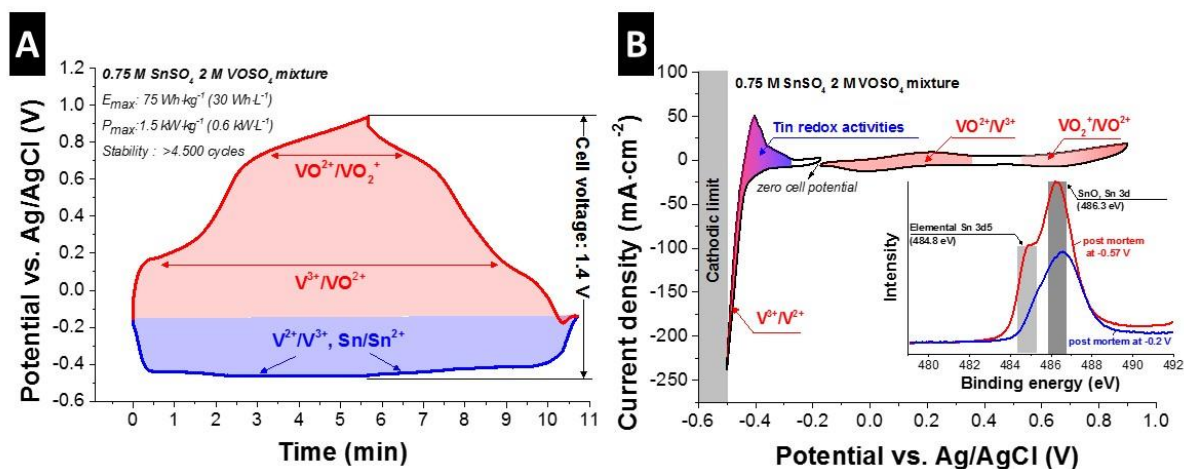


Figure S1: (A) The potential development of the positive and the negative electrodes obtained from 0.75 M SnSO_4 2 M VOSO_4 mixture system in $0.1\text{ M H}_2\text{SO}_4$. (B) The cyclic voltammograms obtained for 0.75 M SnSO_4 2 M VOSO_4 system in $0.1\text{ M H}_2\text{SO}_4$ in the potential range of either the negative or the positive electrode. The inset shows the post mortem XPS data from the negative electrode charged at -0.57 V and -0.2 V . For more information on this system, also see Ref. ¹.

Post mortem analysis of activated carbon electrodes operated with the SnSO_4 - VO_2 redox electrolyte system

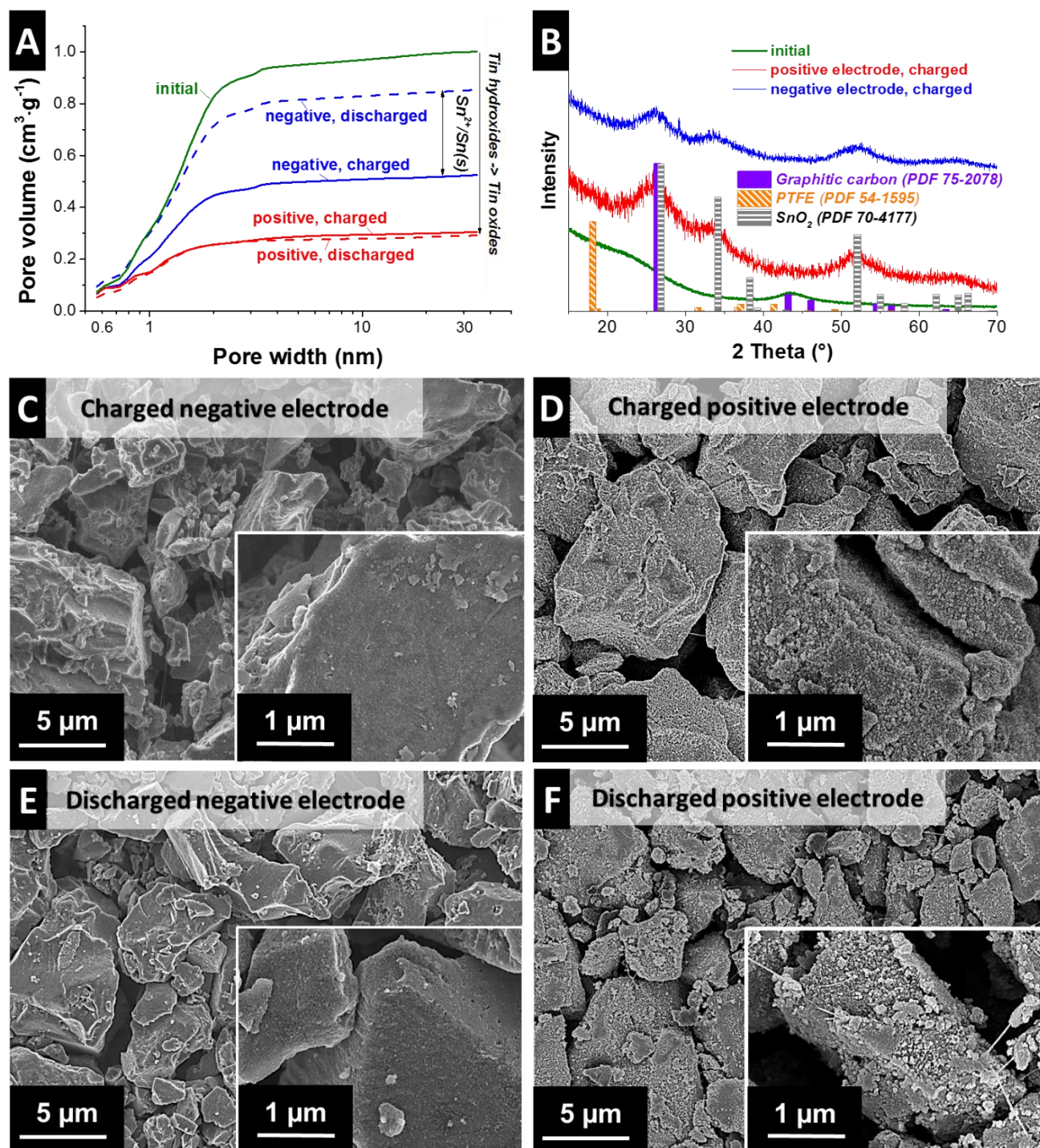


Figure S2: Post mortem analyses of electrodes operated using 0.75 M SnSO_4 2 M VO_2 mixture electrolyte. (A) Pore size distribution pattern calculated by quenched solid density functional theory analysis of nitrogen sorption data. (B) X-ray diffraction patterns. (C-F) Scanning electron micrographs.

Three-electrode experiments (half-cell)

For the three-electrode half-cell experiments, a spring-loaded two-piston cell was used with Ag/AgCl reference electrode (saturated, 3 M NaCl). As current collectors, two graphite pistons were applied for the working and counter electrodes while GF/A glassy fiber filter (Whatman) was located in between to prevent the short circuit and to reserve electrolyte. Working electrode was prepared with 4 mm diameter and 200 μm thickness while a double stack of porous carbon electrode was used as counter electrode (12 mm diameter, 500 μm thickness).

Figure S3B shows the reversible hydrogen storage at the carbon micropores (YP-80F activated carbon bound with 5 mass% PTFE) as the potential is scanned from -0.5 V to +0.6 V. At a potential lower than -0.5 V, hydrogen storage does not seem to be reversible anymore.

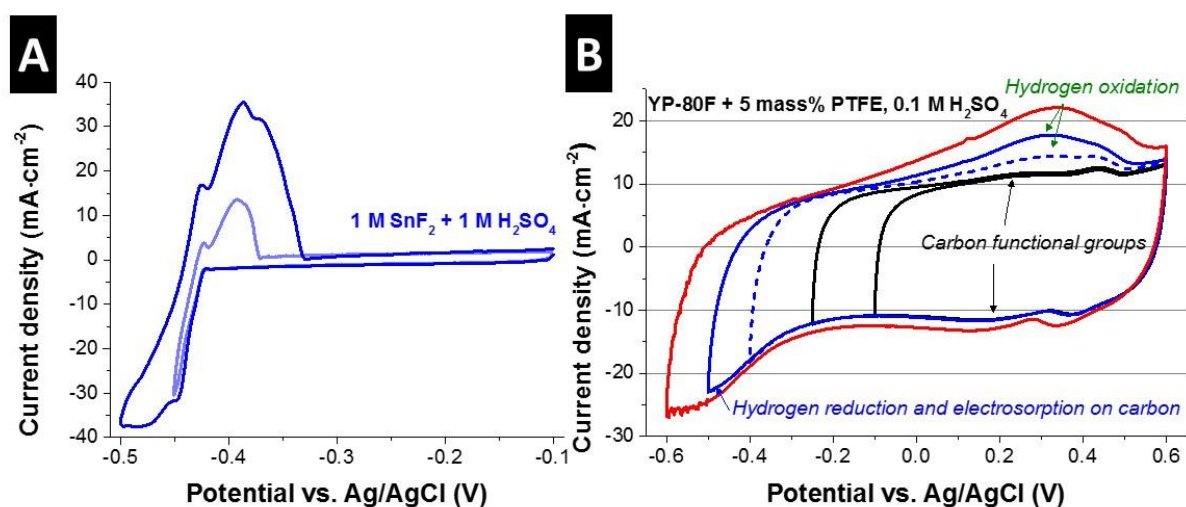


Figure S3: Cyclic voltammograms of 1 M SnF_2 + 1 M H_2SO_4 system (A) and 0.1 M H_2SO_4 system (B) at $1 \text{ mV}\cdot\text{s}^{-1}$.

Rate behavior and the cycling stability test with full cell configuration

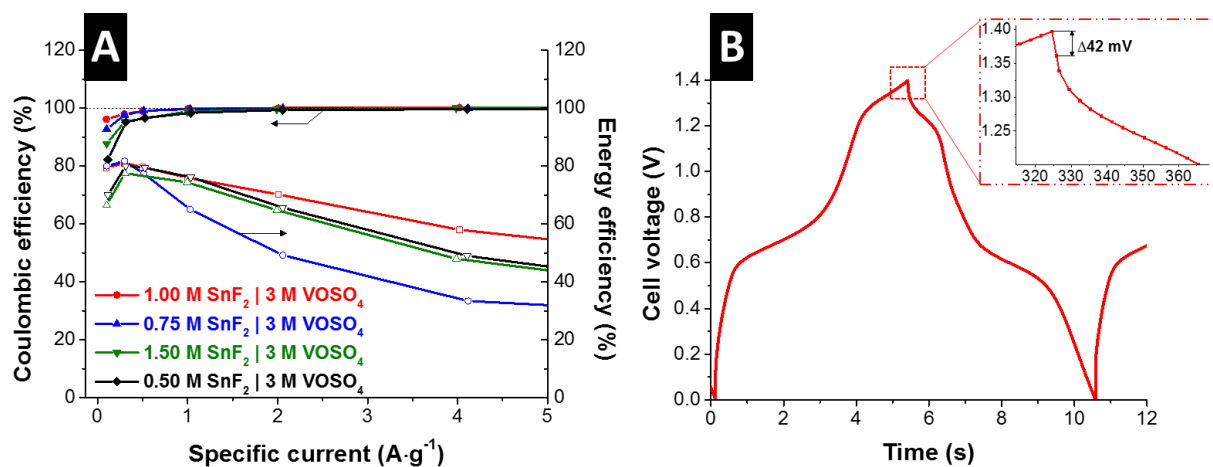


Figure S4: (A) Coulombic and energy efficiency of the asymmetric electrolyte system with SnF_2 and VOSO_4 in 1 M H_2SO_4 at various specific current. (B) GCPL curves obtained after applying 100 cycles at $1 \text{ A}\cdot\text{g}^{-1}$. The inset shows the iR drop.

Ragone plot

For the gravimetric Ragone plot (**Figure S5A**), the values are normalized to the active mass of the electrode excluding the mass of the separator, electrolyte, current collector, and device outer housing. However, this active mass normalization can mislead when the values are compared to that of commercial products which are generally normalized by the total device mass. For a fair comparison, a wet normalization was suggested which considers the mass of the electrolyte and electrode.² The suggested normalization technique requires the skeletal density of the electrode and the electrolyte density which allows the calculation of the electrolyte mass which are confined in porous carbon electrode. Following the procedures described in Ref.², the maximum specific energy for the asymmetric electrolyte system (1 M SnF_2 | 3 M VOSO_4) is calculated to be around $17.2 \text{ Wh}\cdot\text{kg}^{-1}$. On the contrary, when the performance of a double-layer capacitor (1 M Na_2SO_4) is normalized to the mass of the electrode and electrolyte, the specific energy is only about $1.2 \text{ Wh}\cdot\text{kg}^{-1}$.

For the volumetric Ragone plot (**Figure S5B**), the values are normalized to the volume of the electrode, separator, and electrolyte.

For the areal Ragone plot (**Figure S5C**), the values are normalized to the area of the separator in the cell. The specific energy of the asymmetric electrolyte system (1 M SnF_2 | 3 M VOSO_4) is about 12 times higher than that of a double layer capacitor (1 M Na_2SO_4). This indicates that the use of anion exchange membrane is beneficial in terms of specific energy despite its high price as long as the price of the anion exchange membrane does not exceed the 12-fold price of the conventional porous separator applied for double-layer capacitors.

The promising features of the asymmetric electrolyte system (1 M SnF_2 | 3 M VOSO_4) can be seen in all Ragone plots with various normalizations exhibiting significant enhancement for energy storage while keeping a high power performance close to that of a double-layer capacitor (1 M Na_2SO_4).

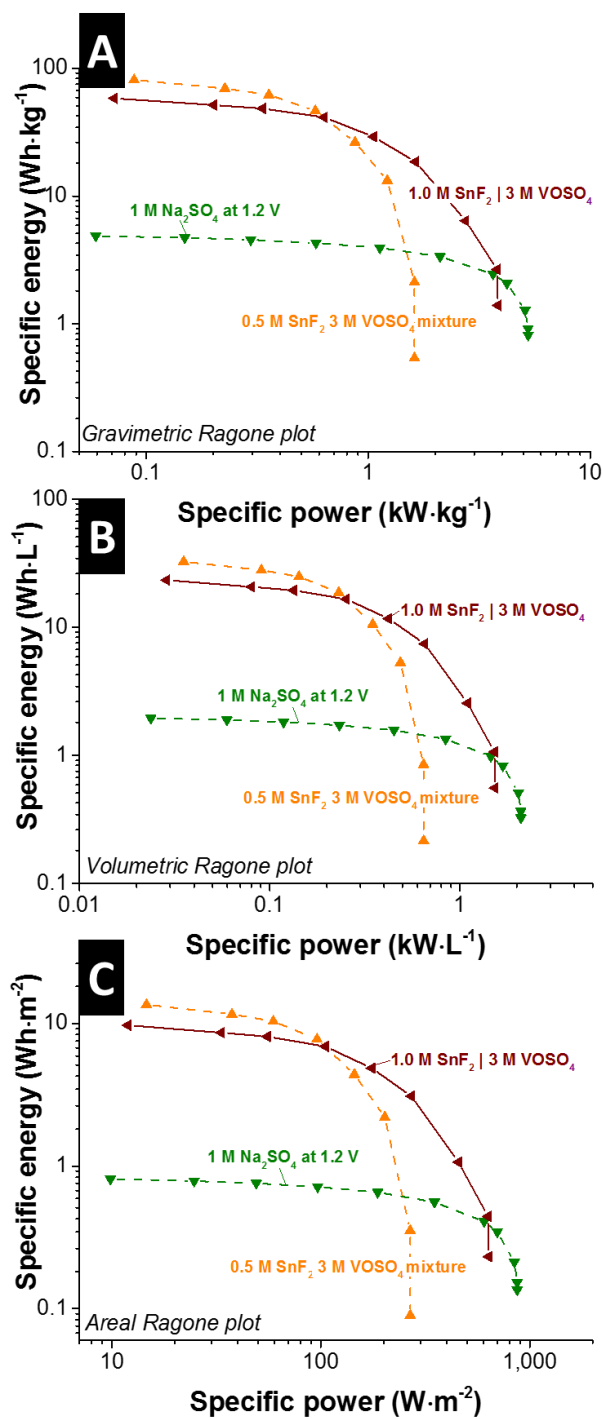


Figure S5: Ragone plot for the comparison of a mixture electrolyte (0.5 M SnF_2 3 M VOSO_4 mixture), asymmetric electrolyte (1 M SnF_2 | 3 M VOSO_4), and a double layer capacitor (1 M Na_2SO_4) with gravimetric (A), volumetric (B), and areal (C) normalization.

Pore distribution from nitrogen gas sorption and thermogravimetric analysis

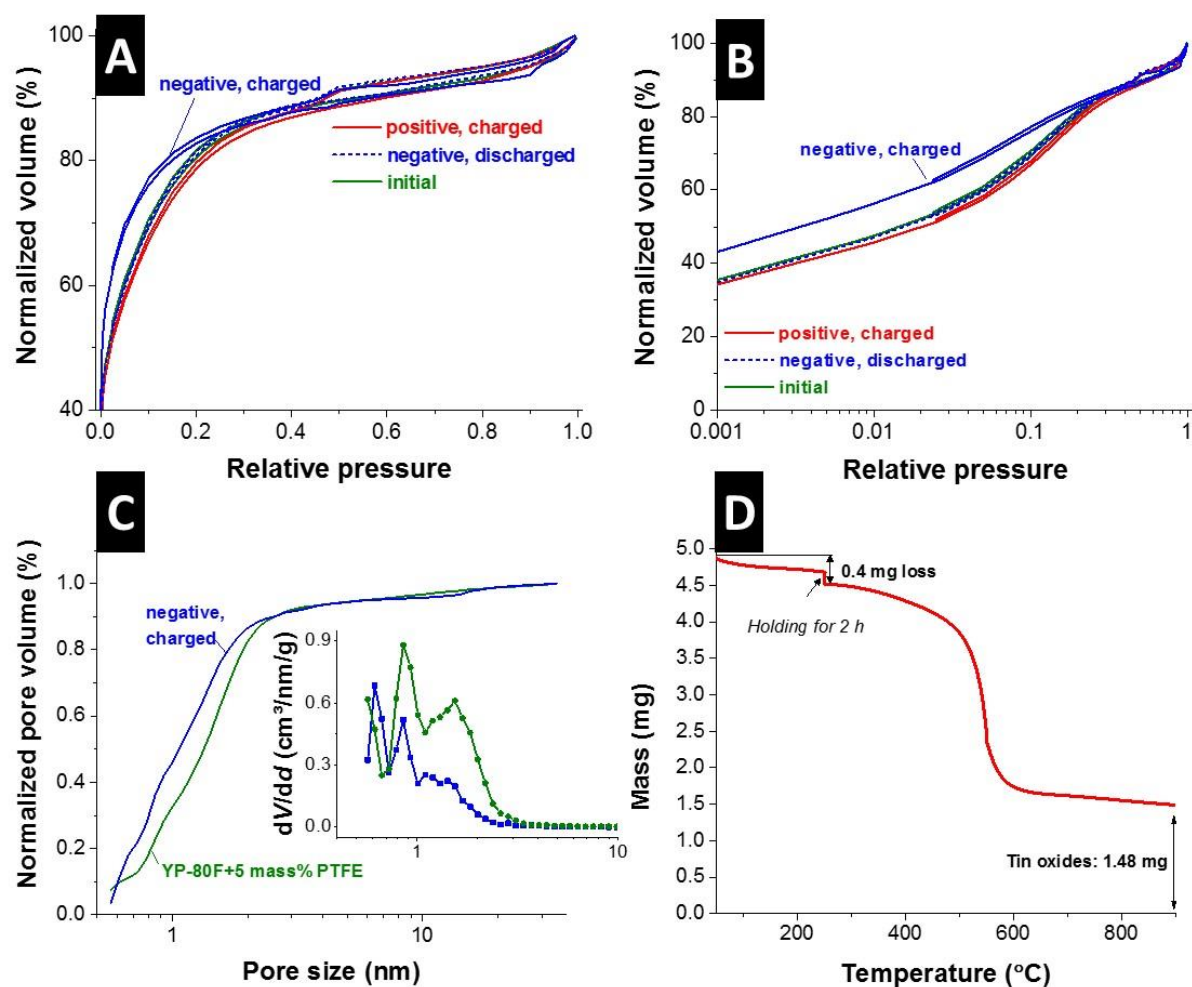


Figure S6: Normalized isotherms in different scales (A-B) and normalized cumulative pore volume vs. pore size plot (C) as normalized to the maximum value of each samples while the inset shows the dV/dd plot. (D) Mass loss data for charged negative electrode from thermogravimetric analysis is plotted as a function of applied temperature. At 200 °C, the temperature was held for 2 h.

Selected area electron diffraction (SAED)

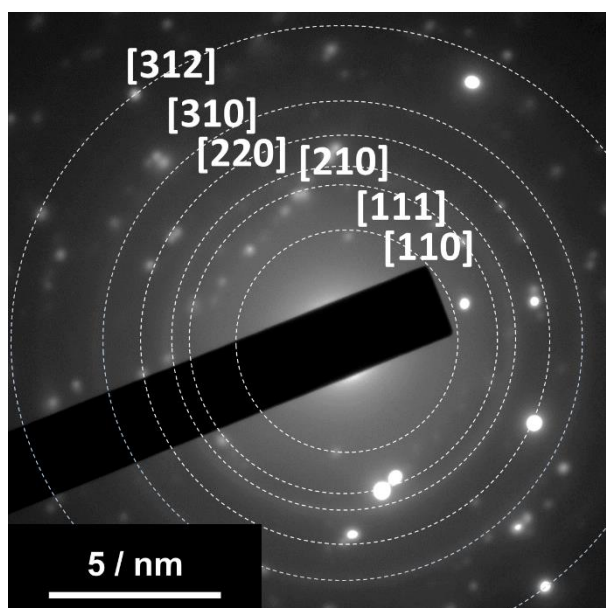


Figure S7: Selective area diffraction patterns obtained for the negative electrode in charged state for 1 M SnF_2 | 3 M VOSO_4 in 1 M H_2SO_4 system. The indices correspond with rutile-type SnO_2 planes.

Supporting references

1. Lee, J.; Krüner, B.; Tolosa, A.; Sathyamoorthi, S.; Kim, D.; Choudhury, S.; Seo, K.-H.; Presser, V., Tin/vanadium redox electrolyte for battery-like energy storage capacity combined with supercapacitor-like power handling. *Energy Environ Sci* **2016**, 9, (11), 3392-3398.
2. Chun, S.-E.; Evanko, B.; Wang, X.; Vonlanthen, D.; Ji, X.; Stucky, G. D.; Boettcher, S. W., Design of aqueous redox-enhanced electrochemical capacitors with high specific energies and slow self-discharge. *Nat Commun* **2015**, 6.